

Measurement of the Inclusive Leptonic Asymmetry in Top-Quark Pairs that Decay to Two Charged Leptons at CDF

- T. Aaltonen,²¹ S. Amerio,^{39a,39b} D. Amidei,³¹ A. Anastassov,^{15,v} A. Annovi,¹⁷ J. Antos,¹² G. Apollinari,¹⁵ J. A. Appel,¹⁵ T. Arisawa,⁵² A. Artikov,¹³ J. Asaadi,⁴⁷ W. Ashmanskas,¹⁵ B. Auerbach,² A. Aurisano,⁴⁷ F. Azfar,³⁸ W. Badgett,¹⁵ T. Bae,²⁵ A. Barbaro-Galtieri,²⁶ V. E. Barnes,⁴³ B. A. Barnett,²³ P. Barria,^{41a,41c} P. Bartos,¹² M. Bauche,^{39a,39b} F. Bedeschi,^{41a} S. Behari,¹⁵ G. Bellettini,^{41a,41b} J. Bellinger,⁵⁴ D. Benjamin,¹⁴ A. Beretvas,¹⁵ A. Bhatti,⁴⁵ K. R. Bland,⁵ B. Blumenfeld,²³ A. Bocci,¹⁴ A. Bodek,⁴⁴ D. Bortoletto,⁴³ J. Boudreau,⁴² A. Boveia,¹¹ L. Brigliadori,^{6a,6b} C. Bromberg,³² E. Brucken,²¹ J. Budagov,¹³ H. S. Budd,⁴⁴ K. Burkett,¹⁵ G. Busetto,^{39a,39b} P. Bussey,¹⁹ P. Butti,^{41a,41b} A. Buzatu,¹⁹ A. Calambra,¹⁰ S. Camarda,⁴ M. Campanelli,²⁸ F. Canelli,^{11,cc} B. Carls,²² D. Carlsmith,⁵⁴ R. Carosi,^{41a} S. Carrillo,^{16,l} B. Casal,^{9,j} M. Casarsa,^{48a} A. Castro,^{6a,6b} P. Catastini,²⁰ D. Cauz,^{48a,48b,48c} V. Cavaliere,²² M. Cavalli-Sforza,⁴ A. Cerri,^{26,e} L. Cerrito,^{28,q} Y. C. Chen,¹ M. Chertok,⁷ G. Chiarelli,^{41a} G. Chlachidze,¹⁵ K. Cho,²⁵ D. Chokheli,¹³ A. Clark,¹⁸ C. Clarke,⁵³ M. E. Convery,¹⁵ J. Conway,⁷ M. Corbo,^{15,y} M. Cordelli,¹⁷ C. A. Cox,⁷ D. J. Cox,⁷ M. Cremonesi,^{41a} D. Cruz,⁴⁷ J. Cuevas,^{9,x} R. Culbertson,¹⁵ N. d'Ascenzo,^{15,u} M. Datta,^{15,ff} P. de Barbaro,⁴⁴ L. Demortier,⁴⁵ M. Deninno,^{6a} M. D'Errico,^{39a,39b} F. Devoto,²¹ A. Di Canto,^{41a,41b} B. Di Ruzza,^{15,p} J. R. Dittmann,⁵ S. Donati,^{41a,41b} M. D'Onofrio,²⁷ M. Dorigo,^{48a,48d} A. Driutti,^{48a,48b,48c} K. Ebina,⁵² R. Edgar,³¹ A. Elagin,⁴⁷ R. Erbacher,⁷ S. Errede,²² B. Esham,²² S. Farrington,³⁸ J. P. Fernández Ramos,²⁹ R. Field,¹⁶ G. Flanagan,^{15,s} R. Forrest,⁷ M. Franklin,²⁰ J. C. Freeman,¹⁵ H. Frisch,¹¹ Y. Funakoshi,⁵² C. Galloni,^{41a,41b} A. F. Garfinkel,⁴³ P. Garosi,^{41a,41c} H. Gerberich,²² E. Gerchtein,¹⁵ S. Giagu,^{46a} V. Giakoumopoulou,³ K. Gibson,⁴² C. M. Ginsburg,¹⁵ N. Giokaris,³ P. Giromini,¹⁷ G. Giurgiu,²³ V. Glagolev,¹³ D. Glenzinski,¹⁵ M. Gold,³⁴ D. Goldin,⁴⁷ A. Golossanov,¹⁵ G. Gomez,⁹ G. Gomez-Ceballos,³⁰ M. Goncharov,³⁰ O. González López,²⁹ I. Gorelov,³⁴ A. T. Goshaw,¹⁴ K. Goulianatos,⁴⁵ E. Gramellini,^{6a} S. Grinstein,⁴ C. Grossi-Pilcher,¹¹ R. C. Group,^{51,15} J. Guimaraes da Costa,²⁰ S. R. Hahn,¹⁵ J. Y. Han,⁴⁴ F. Happacher,¹⁷ K. Hara,⁴⁹ M. Hare,⁵⁰ R. F. Harr,⁵³ T. Harrington-Taber,^{15,m} K. Hatakeyama,⁵ C. Hays,³⁸ J. Heinrich,⁴⁰ S. Henry,⁴⁷ M. Herndon,⁵⁴ A. Hocker,¹⁵ Z. Hong,⁴⁷ W. Hopkins,^{15,f} S. Hou,¹ R. E. Hughes,³⁵ U. Husemann,⁵⁵ M. Hussein,^{32,aa} J. Huston,³² G. Introzzi,^{41a,41e,41f} M. Iori,^{46a,48b} A. Ivanov,^{7,o} E. James,¹⁵ D. Jang,¹⁰ B. Jayatilaka,¹⁵ E. J. Jeon,²⁵ S. Jindariani,¹⁵ M. Jones,⁴³ K. K. Joo,²⁵ S. Y. Jun,¹⁰ T. R. Junk,¹⁵ M. Kambeitz,²⁴ T. Kamon,^{25,47} P. E. Karchin,⁵³ A. Kasmi,⁵ Y. Kato,^{37,n} W. Ketchum,^{11,gg} J. Keung,⁴⁰ B. Kilminster,^{15,cc} D. H. Kim,²⁵ H. S. Kim,²⁵ J. E. Kim,²⁵ M. J. Kim,¹⁷ S. H. Kim,⁴⁹ S. B. Kim,²⁵ Y. J. Kim,²⁵ Y. K. Kim,¹¹ N. Kimura,⁵² M. Kirby,¹⁵ K. Knoepfel,¹⁵ K. Kondo,^{52,*} D. J. Kong,²⁵ J. Konigsberg,¹⁶ A. V. Kotwal,¹⁴ M. Kreps,²⁴ J. Kroll,⁴⁰ M. Kruse,¹⁴ T. Kuhr,²⁴ M. Kurata,⁴⁹ A. T. Laasanen,⁴³ S. Lammel,¹⁵ M. Lancaster,²⁸ K. Lannon,^{35,w} G. Latino,^{41a,41c} H. S. Lee,²⁵ J. S. Lee,²⁵ S. Leo,^{41a} S. Leone,^{41a} J. D. Lewis,¹⁵ A. Limosani,^{14,r} E. Lipeles,⁴⁰ A. Lister,^{18,a} H. Liu,⁵¹ Q. Liu,⁴³ T. Liu,¹⁵ S. Lockwitz,⁵⁵ A. Loginov,⁵⁵ D. Lucchesi,^{39a,39b} A. Lucà,¹⁷ J. Lueck,²⁴ P. Lujan,²⁶ P. Lukens,¹⁵ G. Lungu,⁴⁵ J. Lys,²⁶ R. Lysak,^{12,d} R. Madrak,¹⁵ P. Maestro,^{41a,41c} S. Malik,⁴⁵ G. Manca,^{27,b} A. Manousakis-Katsikakis,³ L. Marchese,^{6a,hh} F. Margaroli,^{46a} P. Marino,^{41a,41d} M. Martínez,⁴ K. Matera,²² M. E. Mattson,⁵³ A. Mazzacane,¹⁵ P. Mazzanti,^{6a} R. McNulty,^{27,i} A. Mehta,²⁷ P. Mehtala,²¹ C. Mesropian,⁴⁵ T. Miao,¹⁵ D. Mietlicki,³¹ A. Mitra,¹ H. Miyake,⁴⁹ S. Moed,¹⁵ N. Moggi,^{6a} C. S. Moon,^{15,y} R. Moore,^{dd,15,ee} M. J. Morello,^{41a,41d} A. Mukherjee,¹⁵ Th. Muller,²⁴ P. Murat,¹⁵ M. Mussini,^{6a,6b} J. Nachtmann,^{15,m} Y. Nagai,⁴⁹ J. Naganoma,⁵² I. Nakano,³⁶ A. Napier,⁵⁰ J. Nett,⁴⁷ C. Neu,⁵¹ T. Nigmanov,⁴² L. Nodulman,² S. Y. Noh,²⁵ O. Norniella,²² L. Oakes,³⁸ S. H. Oh,¹⁴ Y. D. Oh,²⁵ I. Oksuzian,⁵¹ T. Okusawa,³⁷ R. Orava,²¹ L. Ortolan,⁴ C. Pagliarone,^{48a} E. Palencia,^{9,e} P. Palni,³⁴ V. Papadimitriou,¹⁵ W. Parker,⁵⁴ G. Paulette,^{48a,48b,48c} M. Paulini,¹⁰ C. Paus,³⁰ T. J. Phillips,¹⁴ G. Piacentino,^{41a} E. Pianori,⁴⁰ J. Pilot,⁷ K. Pitts,²² C. Plager,⁸ L. Pondrom,⁵⁴ S. Poprocki,^{15,f} K. Potamianos,²⁶ A. Pranko,²⁶ F. Prokoshin,^{13,z} F. Ptahos,^{17,g} G. Punzi,^{41a,41b} N. Ranjan,⁴³ I. Redondo Fernández,²⁹ P. Renton,³⁸ M. Rescigno,^{46a} F. Rimondi,^{6a,*} L. Ristori,^{41a,15} A. Robson,¹⁹ T. Rodriguez,⁴⁰ S. Rolli,^{50,h} M. Ronzani,^{41a,41b} R. Roser,¹⁵ J. L. Rosner,¹¹ F. Ruffini,^{41a,41c} A. Ruiz,⁹ J. Russ,¹⁰ V. Rusu,¹⁵ W. K. Sakamoto,⁴⁴ Y. Sakurai,⁵² L. Santi,^{48a,48b,48c} K. Sato,⁴⁹ V. Saveliev,^{15,u} A. Savoy-Navarro,^{15,y} P. Schlabach,¹⁵ E. E. Schmidt,¹⁵ T. Schwarz,³¹ L. Scodellaro,⁹ F. Scuri,^{41a} S. Seidel,³⁴ Y. Seiya,³⁷ A. Semenov,¹³ F. Sforza,^{41a,41b} S. Z. Shalhout,⁷ T. Shears,²⁷ P. F. Shepard,⁴² M. Shimojima,^{49,t} M. Shochet,¹¹ I. Shreyber-Tecker,³³ A. Simonenko,¹³ K. Sliwa,⁵⁰ J. R. Smith,⁷ F. D. Snider,¹⁵ H. Song,⁴² V. Sorin,⁴ R. St. Denis,^{19,*} M. Stancari,¹⁵ D. Stentz,^{15,v} J. Strologas,³⁴ Y. Sudo,⁴⁹ A. Sukhanov,¹⁵ I. Suslov,¹³ K. Takemasa,⁴⁹ Y. Takeuchi,⁴⁹ J. Tang,¹¹ M. Tecchio,³¹ P. K. Teng,¹ J. Thom,^{15,f} E. Thomson,⁴⁰ V. Thukral,⁴⁷ D. Toback,⁴⁷ S. Tokar,¹² K. Tollefson,³² T. Tomura,⁴⁹ D. Tonelli,^{15,e} S. Torre,¹⁷ D. Torretta,¹⁵ P. Totaro,^{39a} M. Trovato,^{41a,41d} F. Ukegawa,⁴⁹ S. Uozumi,²⁵ F. Vázquez,^{16,l} G. Velev,¹⁵ C. Vellidis,¹⁵ C. Vernieri,^{41a,41d} M. Vidal,⁴³ R. Vilar,⁹ J. Vizán,^{9,bb} M. Vogel,³⁴ G. Volpi,¹⁷ P. Wagner,⁴⁰ R. Wallny,^{15,j} S. M. Wang,¹ D. Waters,²⁸ W. C. Wester III,¹⁵ D. Whiteson,^{40,c} A. B. Wicklund,² S. Wilbur,⁷ H. H. Williams,⁴⁰

J. S. Wilson,³¹ P. Wilson,¹⁵ B. L. Winer,³⁵ P. Wittich,^{15,f} S. Wolbers,¹⁵ H. Wolfe,³⁵ T. Wright,³¹ X. Wu,¹⁸ Z. Wu,⁵ K. Yamamoto,³⁷ D. Yamato,³⁷ T. Yang,¹⁵ U. K. Yang,²⁵ Y. C. Yang,²⁵ W.-M. Yao,²⁶ G. P. Yeh,¹⁵ K. Yi,^{15,m} J. Yoh,¹⁵ K. Yorita,⁵² T. Yoshida,^{37,k} G. B. Yu,¹⁴ I. Yu,²⁵ A. M. Zanetti,^{48a} Y. Zeng,¹⁴ C. Zhou,¹⁴ and S. Zucchelli^{6a,6b}

(CDF Collaboration)

¹Institute of Physics, Academia Sinica, Taipei, Taiwan 11529, Republic of China

²Argonne National Laboratory, Argonne, Illinois 60439, USA

³University of Athens, 157 71 Athens, Greece

⁴Institut de Fisica d'Altes Energies, ICREA, Universitat Autonoma de Barcelona, E-08193 Bellaterra (Barcelona), Spain

⁵Baylor University, Waco, Texas 76798, USA

^{6a}Istituto Nazionale di Fisica Nucleare Bologna, Italy

^{6b}University of Bologna, I-40127 Bologna, Italy

⁷University of California, Davis, Davis, California 95616, USA

⁸University of California, Los Angeles, Los Angeles, California 90024, USA

⁹Instituto de Fisica de Cantabria, CSIC-University of Cantabria, 39005 Santander, Spain

¹⁰Carnegie Mellon University, Pittsburgh, Pennsylvania 15213, USA

¹¹Enrico Fermi Institute, University of Chicago, Chicago, Illinois 60637, USA

¹²Comenius University, 842 48 Bratislava, Slovakia; Institute of Experimental Physics, 040 01 Kosice, Slovakia

¹³Joint Institute for Nuclear Research, RU-141980 Dubna, Russia

¹⁴Duke University, Durham, North Carolina 27708, USA

¹⁵Fermi National Accelerator Laboratory, Batavia, Illinois 60510, USA

¹⁶University of Florida, Gainesville, Florida 32611, USA

¹⁷Laboratori Nazionali di Frascati, Istituto Nazionale di Fisica Nucleare, I-00044 Frascati, Italy

¹⁸University of Geneva, CH-1211 Geneva 4, Switzerland

¹⁹Glasgow University, Glasgow G12 8QQ, United Kingdom

²⁰Harvard University, Cambridge, Massachusetts 02138, USA

²¹Division of High Energy Physics, Department of Physics, University of Helsinki, FIN-00014 Helsinki, Finland;
Helsinki Institute of Physics, FIN-00014 Helsinki, Finland

²²University of Illinois, Urbana, Illinois 61801, USA

²³The Johns Hopkins University, Baltimore, Maryland 21218, USA

²⁴Institut für Experimentelle Kernphysik, Karlsruhe Institute of Technology, D-76131 Karlsruhe, Germany

²⁵Center for High Energy Physics, Kyungpook National University, Daegu 702-701, Korea;

Seoul National University, Seoul 151-742, Korea; Sungkyunkwan University, Suwon 440-746, Korea;

Korea Institute of Science and Technology Information, Daejeon 305-806, Korea;

Chonnam National University, Gwangju 500-757, Korea;

Chonbuk National University, Jeonju 561-756, Korea; and

Ewha Womans University, Seoul 120-750, Korea

²⁶Ernest Orlando Lawrence Berkeley National Laboratory, Berkeley, California 94720, USA

²⁷University of Liverpool, Liverpool L69 7ZE, United Kingdom

²⁸University College London, London WC1E 6BT, United Kingdom

²⁹Centro de Investigaciones Energeticas Medioambientales y Tecnologicas, E-28040 Madrid, Spain

³⁰Massachusetts Institute of Technology, Cambridge, Massachusetts 02139, USA

³¹University of Michigan, Ann Arbor, Michigan 48109, USA

³²Michigan State University, East Lansing, Michigan 48824, USA

³³Institution for Theoretical and Experimental Physics, ITEP, Moscow 117259, Russia

³⁴University of New Mexico, Albuquerque, New Mexico 87131, USA

³⁵The Ohio State University, Columbus, Ohio 43210, USA

³⁶Okayama University, Okayama 700-8530, Japan

³⁷Osaka City University, Osaka 558-8585, Japan

³⁸University of Oxford, Oxford OX1 3RH, United Kingdom

^{39a}Istituto Nazionale di Fisica Nucleare, Sezione di Padova, Italy

^{39b}University of Padova, I-35131 Padova, Italy

⁴⁰University of Pennsylvania, Philadelphia, Pennsylvania 19104, USA

^{41a}Istituto Nazionale di Fisica Nucleare Pisa, Italy

^{41b}University of Pisa, Italy

^{41c}University of Siena, Italy

^{41d}Scuola Normale Superiore, I-56127 Pisa, Italy

^{41e}INFN Pavia, I-27100 Pavia, Italy

^{41f}*University of Pavia, I-27100 Pavia, Italy*⁴²*University of Pittsburgh, Pittsburgh, Pennsylvania 15260, USA*⁴³*Purdue University, West Lafayette, Indiana 47907, USA*⁴⁴*University of Rochester, Rochester, New York 14627, USA*⁴⁵*The Rockefeller University, New York, New York 10065, USA*^{46a}*Istituto Nazionale di Fisica Nucleare, Sezione di Roma 1, Italy*^{46b}*Sapienza Università di Roma, I-00185 Roma, Italy*⁴⁷*Mitchell Institute for Fundamental Physics and Astronomy, Texas A&M University, College Station, Texas 77843, USA*^{48a}*Istituto Nazionale di Fisica Nucleare Trieste, Italy*^{48b}*Gruppo Collegato di Udine, Italy*^{48c}*University of Udine, I-33100 Udine, Italy*^{48d}*University of Trieste, I-34127 Trieste, Italy*⁴⁹*University of Tsukuba, Tsukuba, Ibaraki 305, Japan*⁵⁰*Tufts University, Medford, Massachusetts 02155, USA*⁵¹*University of Virginia, Charlottesville, Virginia 22906, USA*⁵²*Waseda University, Tokyo 169, Japan*⁵³*Wayne State University, Detroit, Michigan 48201, USA*⁵⁴*University of Wisconsin, Madison, Wisconsin 53706, USA*⁵⁵*Yale University, New Haven, Connecticut 06520, USA*

(Received 15 April 2014; published 23 July 2014)

We measure the inclusive forward–backward asymmetry of the charged-lepton pseudorapidities from top-quark pairs produced in proton–antiproton collisions and decaying to final states that contain two charged leptons (electrons or muons). The data are collected with the Collider Detector at Fermilab and correspond to an integrated luminosity of 9.1 fb^{-1} . We measure the leptonic forward–backward asymmetry, A_{FB}^{ℓ} , to be 0.072 ± 0.060 and the leptonic pair forward–backward asymmetry, $A_{\text{FB}}^{\ell\ell}$, to be 0.076 ± 0.082 . The measured values can be compared with the standard model predictions of $A_{\text{FB}}^{\ell} = 0.038 \pm 0.003$ and $A_{\text{FB}}^{\ell\ell} = 0.048 \pm 0.004$, respectively. Additionally, we combine the A_{FB}^{ℓ} result with a previous determination from a final state with a single lepton and hadronic jets and obtain $A_{\text{FB}}^{\ell} = 0.090^{+0.028}_{-0.026}$.

DOI: 10.1103/PhysRevLett.113.042001

PACS numbers: 14.65.Ha, 11.30.Er, 12.38.Qk, 13.85.Qk

One special property of the production of top quark–antitop quark pairs ($t\bar{t}$) in proton–antiproton collisions at the Fermilab Tevatron is the forward–backward asymmetry ($A_{\text{FB}}^{\tilde{t}\tilde{t}}$), which refers to the preference of top quarks to follow the proton direction, forward, and antitop quarks to follow the opposite direction, backward. Recent measurements of $A_{\text{FB}}^{\tilde{t}\tilde{t}}$ [1–3] show deviations from the prediction calculated assuming the standard model (SM) of particle physics [4]. This has triggered substantial interest in the physics community as the SM predicts only small asymmetry due to interference among diagrams starting at next-to-leading order (NLO), while non-SM particles or interactions could modify $A_{\text{FB}}^{\tilde{t}\tilde{t}}$ significantly [5].

A separate set of useful observables relies on the pseudorapidities (η) of the charged leptons that can originate from the cascade decays of the top quarks. These are the asymmetry in the charge-weighted η of the charged lepton (ℓ , where we only consider electrons and muons), the so-called leptonic forward–backward asymmetry (A_{FB}^{ℓ}), and the leptonic pair forward–backward asymmetry ($A_{\text{FB}}^{\ell\ell}$) for the final state with two charged leptons (dilepton final state), defined with the η difference between the two charged leptons [6]. In a hypothetical scenario where $t\bar{t}$ pairs could be produced via a gluon with axial couplings (“axigluon”),

$A_{\text{FB}}^{\tilde{t}\tilde{t}}$ could deviate from its SM value; equally interesting, the various axigluon couplings to the top quarks could result in the same value of $A_{\text{FB}}^{\tilde{t}\tilde{t}}$, but with very different values of A_{FB}^{ℓ} and $A_{\text{FB}}^{\ell\ell}$ [7].

In this Letter, we summarize the measurements of the A_{FB}^{ℓ} and the $A_{\text{FB}}^{\ell\ell}$ in the dilepton final state using the data collected by the CDF II detector during the full Tevatron Run II period, with an integrated luminosity of 9.1 fb^{-1} [8]. These measurements have the experimental advantage of exploiting the precisely measured angles of the lepton trajectories, which simplifies the analysis by not requiring reconstruction of the four-momenta of the top-quark pairs and reduces systematic uncertainties [9]. The measured asymmetries are reported at parton level in that they are corrected for the detector and selection effects and are *inclusive* in that they are extrapolated to the full η range. These measurements are complementary to the previous measurement of A_{FB}^{ℓ} in the final state involving one lepton and jets (lepton + jets final state) [9], as they have a different signal topology, independent background estimation techniques, and an extended lepton η coverage to the high η regime that is most sensitive to beyond-SM scenarios. Additionally, we report on the combined A_{FB}^{ℓ} result from the two final states.

The CDF II detector, described in detail in Ref. [10], is a general-purpose particle detector employing a large charged-particle tracking volume inside a solenoidal magnetic field coaxial with the beam direction, surrounded by calorimeters and muon detectors. We use a cylindrical coordinate system with the origin at the center of the detector, z pointing in the direction of the proton beam, θ and ϕ representing the polar and azimuthal angles, respectively, and $\eta = -\ln \tan(\theta/2)$. The transverse momentum p_T is defined as $p \sin \theta$, and the transverse energy E_T as $E \sin \theta$.

A sample enriched in $t\bar{t}$ events in the dilepton final state ($t\bar{t} \rightarrow \ell^+ \ell^- \nu \bar{\nu} b\bar{b}$) is selected by requiring two oppositely charged leptons, two or more narrow clusters of energy deposits in the calorimeters, corresponding to collimated clusters of incident hadrons (jets), and an imbalance in the total event transverse momentum (missing transverse energy [11], or E_T) that is consistent with the presence of two neutrinos. Specifically, we require events to pass the same requirements that were used in the measurement of the $t\bar{t}$ cross section [12], except that we release the requirement that at least one jet has the signature of originating from b -quark fragmentation [13], and raise the minimum dilepton invariant mass requirement from 5 to 10 GeV/c^2 to reduce background modeling uncertainties.

Several physical processes mimic the signature of top-quark pairs in the dilepton final state, such as production of a Z boson or a virtual photon with jets (Z/γ^* + jets), production of a W boson with jets (W + jets), diboson production (WW , WZ , ZZ , and $W\gamma$), and $t\bar{t}$ production where one of the W bosons from the top-quark pair decays hadronically and one jet from bottom-quark hadronization or W -boson hadronic decay is misidentified as a lepton ($t\bar{t}$ nondilepton). The estimation of background and SM $t\bar{t}$ signal is based on the methods of Ref. [12], which exploits both Monte Carlo (MC) simulations and data-based techniques. For the simulations, leading-order event generators are configured to use the CTEQ6.1L set of parton-distribution functions, while NLO event generators use CTEQ6.1M. PYTHIA [14] is used to model the parton hadronization; a GEANT-based simulation [15,16] is used to model the detector response. A $t\bar{t}$ sample to estimate signal and the $t\bar{t}$ nondilepton background is generated with a top-quark mass of 172.5 GeV/c^2 using the POWHEG generator [17–20] and is normalized to the theoretical cross section of 7.4 pb [21]. The expected rates of background processes and the signal, together with the observed number of events selected from data, are listed in Table I. Excellent agreement is observed.

Assuming charge-parity symmetry, the A_{FB}^ℓ can be defined combining leptons of both charges [9] as

$$A_{FB}^\ell = \frac{N(q_\ell \eta_\ell > 0) - N(q_\ell \eta_\ell < 0)}{N(q_\ell \eta_\ell > 0) + N(q_\ell \eta_\ell < 0)}, \quad (1)$$

TABLE I. Expected number of events in data along with the observed number of events, passing all event selections. The quoted uncertainties in each row are the total uncertainties calculated in the same way as Ref. [12].

Source	Events
Diboson	31 ± 6
Z/γ^* + jets	50 ± 6
W + jets	64 ± 17
$t\bar{t}$ nondilepton	14.6 ± 0.8
Total background	160 ± 21
$t\bar{t}$ ($\sigma = 7.4$ pb)	408 ± 19
Total SM expectation	568 ± 40
Observed	569

where N is the number of leptons, q_ℓ is the lepton electric charge, and η_ℓ is the lepton pseudorapidity. Studies of the correlation between the two charged leptons show negligible effect on the measurement. An NLO SM calculation with both quantum-chromodynamics effects and electroweak effects predicts $A_{FB}^\ell = 0.038 \pm 0.003$ [4]. If the genuine value of $A_{FB}^{\tilde{\ell}}$ would be that measured by the CDF collaboration [1], the predicted value for A_{FB}^ℓ for top quarks decaying according to the SM would be $0.070 < A_{FB}^\ell < 0.076$ [9]. Previous measurements of A_{FB}^ℓ in the lepton + jets final state by the CDF collaboration and in the lepton+jets and dilepton final states by the D0 collaboration found $0.094^{+0.032}_{-0.029}$ [9] and 0.047 ± 0.027 [22,23], respectively. A second observable, $A_{FB}^{\ell\ell}$, can be defined in the dilepton final state analogously to $A_{FB}^{\tilde{\ell}}$ as

$$A_{FB}^{\ell\ell} = \frac{N(\Delta\eta > 0) - N(\Delta\eta < 0)}{N(\Delta\eta > 0) + N(\Delta\eta < 0)}, \quad (2)$$

where $\Delta\eta = \eta_{\ell^+} - \eta_{\ell^-}$. An NLO SM prediction yields $A_{FB}^{\ell\ell} = 0.048 \pm 0.004$ [4]. The D0 collaboration measured $A_{FB}^{\ell\ell} = 0.123 \pm 0.056$ [22].

We simulate $t\bar{t}$ production and decay in various plausible SM and beyond-SM scenarios to study hypothetical variations in the expected $q_\ell \eta_\ell$ spectrum. The benchmark SM $t\bar{t}$ sample generated with POWHEG gives parton-level inclusive values of $A_{FB}^\ell = 0.024$ and $A_{FB}^{\ell\ell} = 0.030$. These predictions are different from the NLO SM calculation in Ref. [4] since the simulation does not account for the electroweak corrections [24]. We studied a large number of beyond-SM scenarios with axigluons of a wide variety of masses (200–2000 GeV/c^2) and different couplings to the quarks using MADGRAPH [25]. Of particular interest are a class of relatively light and wide axigluons (with masses at 200 GeV/c^2 and widths at 50 GeV) with left-handed, right-handed, and axial axigluon couplings to the quarks [7]. Each predicts an $A_{FB}^{\tilde{\ell}}$ value similar to that observed by the CDF collaboration [1], but the polarization of the top quarks results in different values of A_{FB}^ℓ (-0.063 , 0.050 , and 0.151 , respectively) and $A_{FB}^{\ell\ell}$ (-0.092 , 0.066 , and

0.218, respectively). Thus, our simulations effectively span a reasonable model space, as well as a final observable range that is wide and centered on the SM-expected value.

Because of the limited detector coverage ($|\eta_l| < 2.0$ for electrons and $|\eta_l| < 1.1$ for muons), imperfect detector acceptance, and contamination from background sources, a correction and extrapolation procedure is needed to determine the parton-level inclusive A_{FB}^ℓ from the data. Studies with the various simulated samples, including the models listed above as well as SM samples generated with PYTHIA [14] and ALPGEN [26], show that the $q_\ell \eta_\ell$ distribution of the leptons at parton level approximately follows the sum of two Gaussian distributions with common means and widths and proportions independent of the simulated model [27]. The asymmetry in each scenario arises from the shift of the mean of the $q_\ell \eta_\ell$ distribution. Using this knowledge, we follow a procedure that is similar to that described in Ref. [9] to account for the detector coverage, detector acceptance, and background effects described above. The $q_\ell \eta_\ell$ distribution of leptons is decomposed into a symmetric part and an asymmetric part as functions of $q_\ell \eta_\ell$ in the range $q_\ell \eta_\ell \geq 0$,

$$\mathcal{S}(q_\ell \eta_\ell) = \frac{\mathcal{N}(q_\ell \eta_\ell) + \mathcal{N}(-q_\ell \eta_\ell)}{2} \quad (3a)$$

and

$$\mathcal{A}(q_\ell \eta_\ell) = \frac{\mathcal{N}(q_\ell \eta_\ell) - \mathcal{N}(-q_\ell \eta_\ell)}{\mathcal{N}(q_\ell \eta_\ell) + \mathcal{N}(-q_\ell \eta_\ell)}, \quad (3b)$$

where $\mathcal{N}(q_\ell \eta_\ell)$ represents the number of events as a function of $q_\ell \eta_\ell$. The differential contribution to the inclusive A_{FB}^ℓ as a function of $q_\ell \eta_\ell$ is calculated as

$$\frac{\mathcal{S}(q_\ell \eta_\ell) \mathcal{A}(q_\ell \eta_\ell)}{\int_0^\infty d(q'_\ell \eta'_\ell) \mathcal{S}(q'_\ell \eta'_\ell)}, \quad (4)$$

and the inclusive A_{FB}^ℓ defined in Eq. (1) is then written as the integral of Eq. (4),

$$A_{FB}^\ell = \frac{\int_0^\infty d(q_\ell \eta_\ell) \mathcal{S}(q_\ell \eta_\ell) \mathcal{A}(q_\ell \eta_\ell)}{\int_0^\infty d(q'_\ell \eta'_\ell) \mathcal{S}(q'_\ell \eta'_\ell)}. \quad (5)$$

The measurement methodology is simplified because the symmetric part of the $q_\ell \eta_\ell$ distributions at parton level is very similar across models as the mean of the $q_\ell \eta_\ell$ distribution is always close to zero in all models and small compared to the width, which is always around unity. We observe that using the distribution from any simulated sample only introduces an uncertainty that is tiny compared to the dominant uncertainties. The methodology also benefits from the fact that the symmetric part of the detector acceptance effect is canceled out in Eq. (3b). Since the detector acceptance, including the effects caused

by lepton reconstruction, behaves in a symmetric way in the dilepton final state, no detector acceptance corrections are found to be needed as in Ref. [9]. Additionally, the differential asymmetry described in Eq. (3b) is readily measured and allows for discrimination among models with different values of A_{FB}^ℓ . For $q_\ell \eta_\ell < 2.5$, the differential asymmetry in Eq. (3b) is modeled accurately by the simplified functional form

$$\mathcal{A}(q_\ell \eta_\ell) = a \cdot \tanh\left(\frac{q_\ell \eta_\ell}{2}\right), \quad (6)$$

where a is the only free parameter related to A_{FB}^ℓ .

Figure 1 shows the differential contribution to the inclusive A_{FB}^ℓ expected at parton level from the POWHEG simulation, along with comparisons to predictions from the two-Gaussian model and the functional form of Eq. (6). Both models describe the distribution accurately. The integral gives the total inclusive asymmetry. The fraction of the unmeasured asymmetry where $|q_\ell \eta_\ell| > 2.0$ is approximately 11%. The shapes of this distribution for all of the simulated samples are very similar, supporting the methodology.

The strategy is to measure the shape of the asymmetric component of the data after background subtraction and use the symmetric component of the parton-level $q_\ell \eta_\ell$ distribution from the POWHEG $t\bar{t}$ sample to reproduce the parton-level inclusive value of A_{FB}^ℓ . This method includes the correction for the acceptance of the detected leptons and extrapolation for the undetected ones. It is validated using the SM and beyond-SM physics scenarios. For both the two-Gaussian model and the simplified functional form of Eq. (6), the method returns A_{FB}^ℓ values that are consistent with the parton-level inclusive values. The most significant discrepancy is assigned as the asymmetric-modeling systematic uncertainty, which is ± 0.006 and covers any possible bias observed.

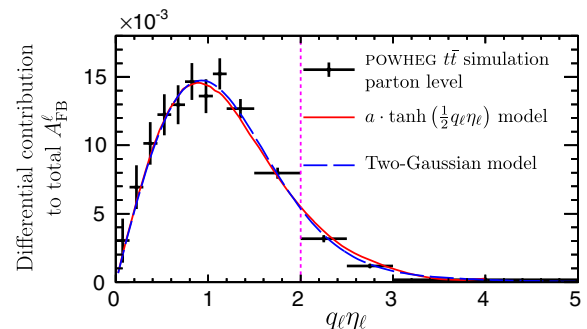


FIG. 1 (color online). Differential contribution to A_{FB}^ℓ for the POWHEG simulation of $t\bar{t}$ production. The solid curve shows the estimation with Eq. (4) where $\mathcal{A}(q_\ell \eta_\ell)$ is obtained with a fit of Eq. (6) on the asymmetric part of the $q_\ell \eta_\ell$ spectrum from the sample and $\mathcal{S}(q_\ell \eta_\ell)$ is directly from the sample; the dashed curve is from the two-Gaussian model [27]. The vertical dashed line indicates the outer limits of the acceptance regions for charged leptons, which is $|q_\ell \eta_\ell| = 2.0$.

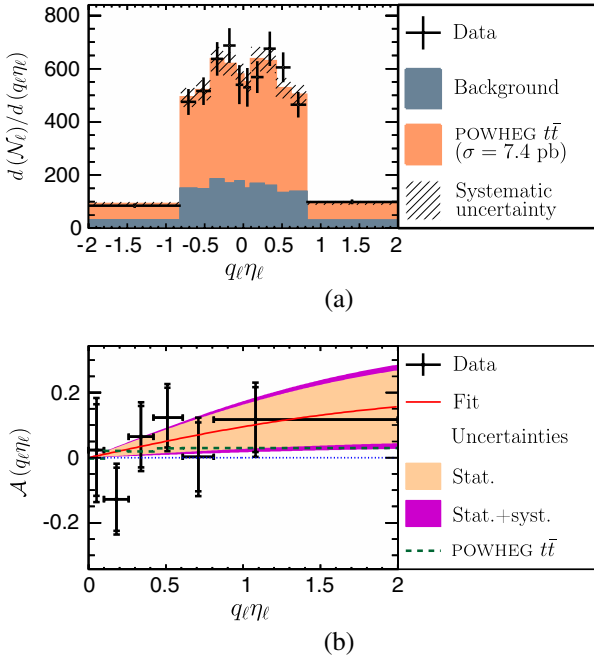


FIG. 2 (color online). (a) Comparison of the observed distribution of $q_\ell\eta_\ell$ with the SM expectations. (b) Asymmetric part of the distribution in (a) defined in Eq. (3b) from data after background subtraction together with the best fit with Eq. (6) and the expectations from the POWHEG MC model. The data points in (b) are placed at the bin centroids predicted by the POWHEG simulation. The inner bars on the data points represent the statistical uncertainties, while the outer bars represent the total uncertainties. The bands indicate the one standard deviation region for statistical and statistical + systematic uncertainties.

The observed distribution of $q_\ell\eta_\ell$ is shown in Fig. 2(a) along with the SM expectations from the $t\bar{t}$ signal and backgrounds. The shapes are well described by the expectations. Figure 2(b) shows the asymmetric component of the data after background subtraction along with the best fit description, which yields a value of $a = 0.21 \pm 0.15$ (stat). Applying Eq. (5), we find $A_{FB}^\ell = 0.072 \pm 0.052$ (stat).

The dominant source of systematic uncertainty is due to the background uncertainties and is estimated to be ± 0.029 using pseudoexperiments [9], which covers both the uncertainties in the background normalizations and the uncertainties in modeling the A_{FB}^ℓ of the backgrounds (including $t\bar{t}$ in nondilepton final state). The next most important source of systematic uncertainty is the ± 0.006 asymmetric-modeling contribution discussed above. The jet-energy-scale systematic uncertainty is estimated to be ± 0.004 by varying the jet energies within their uncertainties. The variations obtained by using the symmetric model from various MC samples are assigned as the symmetric-modeling systematic uncertainty, which is ± 0.001 . Other sources of uncertainties due to the uncertainties in the parton showering model, the modeling of color reconnection, the amount of initial-state and final-state radiation,

and the uncertainty on the parton-distribution functions are found to be negligible. The total systematic uncertainty, ± 0.03 , is estimated by summing the individual contributions in quadrature. The final result is $a = 0.21 \pm 0.15$ (stat) ± 0.08 (syst) and $A_{FB}^\ell = 0.072 \pm 0.052$ (stat) ± 0.030 (syst). This result is consistent with the NLO SM expectation, the measurement in the lepton + jets final state by the CDF collaboration [9] and the measurement by the D0 collaboration [22,23].

Identical methodology is used for measuring A_{FB}^ℓ . The observed distribution of $\Delta\eta$ is shown in Fig. 3. We measure $a = 0.16 \pm 0.15$ (stat) ± 0.08 (syst) and $A_{FB}^\ell = 0.072 \pm 0.072$ (stat) ± 0.039 (syst), where the dominant systematic uncertainty is from backgrounds and has a value of ± 0.037 . The asymmetric- and symmetric-modeling systematic uncertainties are estimated to be ± 0.012 and ± 0.004 , respectively. The jet-energy-scale systematic uncertainty is estimated to be ± 0.003 . Other systematic uncertainties are negligible. This result is consistent with both the NLO SM calculation [4] and the measurement by the D0 collaboration [22].

In order to obtain a more sensitive measurement, we combine the dilepton measurement of A_{FB}^ℓ with the CDF measurement in the lepton + jets final state reported in Ref. [9], $A_{FB}^\ell = 0.094 \pm 0.024$ (stat) $^{+0.022}_{-0.017}$ (syst). The combination is based on the asymmetric iterative algorithm of the “best linear unbiased estimates approach” [28,29]. Since the measurements use statistically independent samples, the statistical uncertainties are uncorrelated. The background systematic uncertainties are treated as uncorrelated since they are mainly caused by the

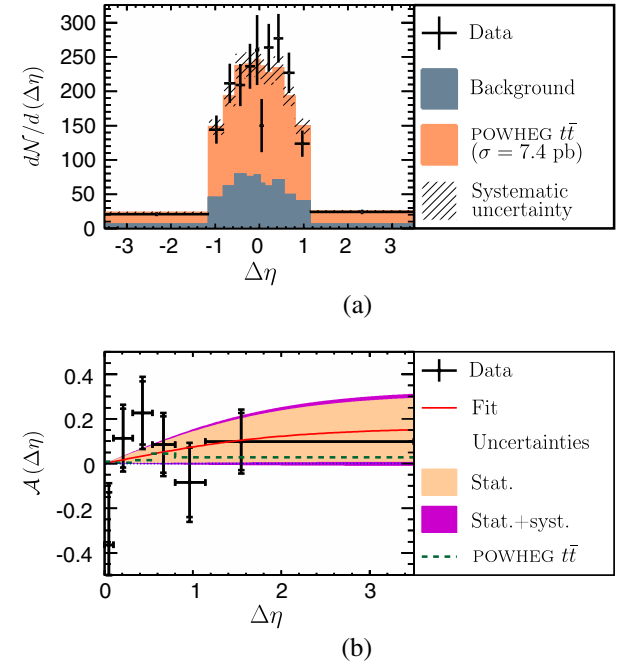


FIG. 3 (color online). The same figures as Fig. 2, but with $\Delta\eta$ instead of $q_\ell\eta_\ell$.

uncertainties in the modeling of the background $q_\ell \eta_\ell$ distributions, which are largely uncorrelated between the two measurements. The recoil-modeling systematic uncertainty in the lepton + jets measurement and the asymmetric-modeling systematic uncertainty in the dilepton measurement (which includes the systematic uncertainty of recoil modeling) are treated as fully correlated. The jet-energy-scale systematic uncertainties are also treated as fully correlated. The other systematic uncertainties are negligible in one of the two measurements; thus, only the non-negligible part is included.

The combined result is $A_{\text{FB}}^\ell = 0.090^{+0.028}_{-0.026}$, where 80% of the measurement weight is due to the lepton + jets result and 20% is due to the dilepton result. The difference in the weights is mostly due to the larger size of the lepton + jets final state sample. The correlation factor between the two measurements is estimated to be 2.6%.

In conclusion, we measure the parton-level inclusive leptonic forward–backward asymmetry and leptonic pair asymmetry of top-quark pairs decaying into the dilepton final state using the full CDF Run II data set. The results are $A_{\text{FB}}^\ell = 0.072 \pm 0.060$ and $A_{\text{FB}}^{\ell\ell} = 0.076 \pm 0.082$, both consistent with previous determinations and expectations. A combination of the CDF A_{FB}^ℓ measurements yields $A_{\text{FB}}^\ell = 0.090^{+0.028}_{-0.026}$. This result is about two standard deviations larger than the NLO SM calculation of $A_{\text{FB}}^\ell = 0.038 \pm 0.003$ [4] but is consistent with the 0.070–0.076 range expected assuming unpolarized top-quark production and SM top-quark decay, given the measured value of $A_{\text{FB}}^{t\bar{t}}$ by the CDF collaboration [9].

We thank the Fermilab staff and the technical staffs of the participating institutions for their vital contributions. This work was supported by the U.S. Department of Energy and National Science Foundation; the Italian Istituto Nazionale di Fisica Nucleare; the Ministry of Education, Culture, Sports, Science and Technology of Japan; the Natural Sciences and Engineering Research Council of Canada; the National Science Council of the Republic of China; the Swiss National Science Foundation; the A.P. Sloan Foundation; the Bundesministerium für Bildung und Forschung, Germany; the Korean World Class University Program, the National Research Foundation of Korea; the Science and Technology Facilities Council and the Royal Society, United Kingdom; the Russian Foundation for Basic Research; the Ministerio de Ciencia e Innovación, and Programa Consolider-Ingenio 2010, Spain; the Slovak R&D Agency; the Academy of Finland; the Australian Research Council (ARC); and the EU community Marie Curie Fellowship Contract No. 302103.

^{*}Deceased.

^aVisitor from University of British Columbia, Vancouver, BC V6T 1Z1, Canada.

^bVisitor from Istituto Nazionale di Fisica Nucleare, Sezione di Cagliari, 09042 Monserrato (Cagliari), Italy.

^cVisitor from University of California Irvine, Irvine, CA 92697, USA.

^dVisitor from Institute of Physics, Academy of Sciences of the Czech Republic, 182 21, Czech Republic.

^eVisitor from CERN, CH-1211 Geneva, Switzerland.

^fVisitor from Cornell University, Ithaca, NY 14853, USA.

^gVisitor from University of Cyprus, Nicosia CY-1678, Cyprus.

^hVisitor from Office of Science, U.S. Department of Energy, Washington, DC 20585, USA.

ⁱVisitor from University College Dublin, Dublin 4, Ireland.

^jVisitor from ETH, 8092 Zürich, Switzerland.

^kVisitor from University of Fukui, Fukui City, Fukui Prefecture 910-0017, Japan.

^lVisitor from Universidad Iberoamericana, Lomas de Santa Fe, México C.P. 01219, Distrito Federal, Mexico.

^mVisitor from University of Iowa, Iowa City, IA 52242, USA.

ⁿVisitor from Kinki University, Higashi-Osaka City 577-8502, Japan.

^oVisitor from Kansas State University, Manhattan, KS 66506, USA.

^pVisitor from Brookhaven National Laboratory, Upton, NY 11973, USA.

^qVisitor from Queen Mary, University of London, London E1 4NS, United Kingdom.

^rVisitor from University of Melbourne, Victoria 3010, Australia.

^sVisitor from Muons, Inc., Batavia, IL 60510, USA.

^tVisitor from Nagasaki Institute of Applied Science, Nagasaki 851-0193, Japan.

^uVisitor from National Research Nuclear University, Moscow 115409, Russia.

^vVisitor from Northwestern University, Evanston, IL 60208, USA.

^wVisitor from University of Notre Dame, Notre Dame, IN 46556, USA.

^xVisitor from Universidad de Oviedo, E-33007 Oviedo, Spain.

^yVisitor from CNRS-IN2P3, Paris F-75205, France.

^zVisitor from Universidad Tecnica Federico Santa Maria, 110v Valparaiso, Chile.

^{aa}Visitor from The University of Jordan, Amman 11942, Jordan.

^{bb}Visitor from Université catholique de Louvain, 1348 Louvain-La-Neuve, Belgium.

^{cc}Visitor from University of Zürich, 8006 Zürich, Switzerland.

^{dd}Visitor from Massachusetts General Hospital, Boston, MA 02114, USA.

^{ee}Visitor from Harvard Medical School, Boston, MA 02114, USA.

^{ff}Visitor from Hampton University, Hampton, VA 23668, USA.

^{gg}Visitor from Los Alamos National Laboratory, Los Alamos, NM 87544, USA.

^{hh}Visitor from Università degli Studi di Napoli Federico I, I-80138 Napoli, Italy.

- [1] T. Aaltonen *et al.* (CDF Collaboration), *Phys. Rev. D* **87**, 092002 (2013).
- [2] V. Abazov *et al.* (D0 Collaboration), arXiv:1405.0421.
- [3] T. Aaltonen *et al.* (CDF Collaboration), *Phys. Rev. Lett.* **111**, 182002 (2013).
- [4] W. Bernreuther and Z.-G. Si, *Phys. Rev. D* **86**, 034026 (2012).
- [5] D.-W. Jung, P. Ko, and J. S. Lee, *Phys. Lett. B* **701**, 248 (2011); D.-W. Jung, P. Ko, J. S. Lee, and S. hyeon Nam, *Phys. Lett. B* **691**, 238 (2010); P. H. Frampton, J. Shu, and K. Wang, *Phys. Lett. B* **683**, 294 (2010); E. Álvarez, L. Rold, and A. Szynkman, *J. High Energy Phys.* 05 (2011) 070; C.-H. Chen, G. Cvetic, and C. Kim, *Phys. Lett. B* **694**, 393 (2011); Y.-k. Wang, B. Xiao, and S.-h. Zhu, *Phys. Rev. D* **82**, 094011 (2010); A. Djouadi, G. Moreau, F. Richard, and R. K. Singh, *Phys. Rev. D* **82**, 071702 (2010); R. S. Chivukula, E. H. Simmons, and C.-P. Yuan, *Phys. Rev. D* **82**, 094009 (2010); B. Xiao, Y.-k. Wang, and S.-h. Zhu, *Phys. Rev. D* **82**, 034026 (2010); Q.-H. Cao, D. McKeen, J. L. Rosner, G. Shaughnessy, and C. E. M. Wagner, *Phys. Rev. D* **81**, 114004 (2010); I. Doršner, S. Fajfer, J. F. Kamenik, and N. Košnik, *Phys. Rev. D* **81**, 055009 (2010); S. Jung, H. Murayama, A. Pierce, and J. D. Wells, *Phys. Rev. D* **81**, 015004 (2010); J. Shu, T. M. P. Tait, and K. Wang, *Phys. Rev. D* **81**, 034012 (2010); A. Arhrib, R. Benbrik, and C.-H. Chen, *Phys. Rev. D* **82**, 034034 (2010); J. Cao, Z. Heng, L. Wu, and J. M. Yang, *Phys. Rev. D* **81**, 014016 (2010); V. Barger, W.-Y. Keung, and C.-T. Yu, *Phys. Rev. D* **81**, 113009 (2010); P. Ferrario and G. Rodrigo, *Phys. Rev. D* **78**, 094018 (2008); **80**, 051701 (2009); M. Bauer, F. Goertz, U. Haisch, T. Pfoh, and S. Westhoff, *J. High Energy Phys.* 11 (2010) 039; K. Cheung, W.-Y. Keung, and T.-C. Yuan, *Phys. Lett. B* **682**, 287 (2009).
- [6] W. Bernreuther and Z.-G. Si, *Nucl. Phys.* **B837**, 90 (2010).
- [7] A. Falkowski, M. L. Mangano, A. Martin, G. Perez, and J. Winter, *Phys. Rev. D* **87**, 034039 (2013).
- [8] Z. Hong, Ph.D. thesis, Texas A&M University [Institution Report No. FERMILAB-THESIS-2014-05] (2014).
- [9] T. Aaltonen *et al.* (CDF Collaboration), *Phys. Rev. D* **88**, 072003 (2013).
- [10] D. Acosta *et al.* (CDF Collaboration), *Phys. Rev. D* **71**, 032001 (2005).
- [11] The missing transverse energy E_T is defined to be $-\sum_i E_T^i \hat{n}_i$ where i identifies the calorimeter tower with $|\eta| < 3.6$ is a unit vector perpendicular to the beam axis and pointing at the i th calorimeter tower.
- [12] T. Aaltonen *et al.* (CDF Collaboration), *Phys. Rev. D* **88**, 091103 (2013).
- [13] D. Acosta *et al.* (CDF Collaboration), *Phys. Rev. D* **71**, 052003 (2005).
- [14] T. Sjostrand, S. Mrenna, and P. Z. Skands, *J. High Energy Phys.* 05 (2006) 026.
- [15] E. Gerchtein and M. Paulini, *Computing in High Energy and Nuclear Physics 2003 Conference Proceedings* eConf C0303241, TUMT005 (2003).
- [16] R. Brun, F. Bruyant, M. Maire, A. McPherson, and P. Zanarini, GEANT3, CERN Report No. CERN-DD-EE-84-1, 1987.
- [17] S. Frixione, P. Nason, and G. Ridolfi, *J. High Energy Phys.* 09 (2007) 126.
- [18] P. Nason, *J. High Energy Phys.* 11 (2004) 040.
- [19] S. Frixione, P. Nason, and C. Oleari, *J. High Energy Phys.* 11 (2007) 070.
- [20] S. Alioli, P. Nason, C. Oleari, and E. Re, *J. High Energy Phys.* 06 (2010) 043.
- [21] M. Czakon and A. Mitov, arXiv:1112.5675.
- [22] V. Abazov *et al.* (D0 Collaboration), *Phys. Rev. D* **88**, 112002 (2013).
- [23] V. Abazov *et al.* (D0 Collaboration), arXiv:1403.1294.
- [24] J. Kühn and G. Rodrigo, *J. High Energy Phys.* 01 (2012) 063; A. V. Manohar and M. Trott, *Phys. Lett. B* **711**, 313 (2012); W. Hollik and D. Pagani, *Phys. Rev. D* **84**, 093003 (2011).
- [25] J. Alwall, P. Demin, S. de Visscher, R. Frederix, M. Herquet, F. Maltoni, T. Plehn, D. L. Rainwater, and T. Stelzer, *J. High Energy Phys.* 09 (2007) 028.
- [26] M. L. Mangano, M. Moretti, F. Piccinini, R. Pittau, and A. D. Polosa, *J. High Energy Phys.* 07 (2003) 001.
- [27] Z. Hong, R. Edgar, S. Henry, D. Toback, J. S. Wilson, and D. Amidei, *Phys. Rev. D* **90**, 014040 (2014).
- [28] L. Lyons, D. Gibaut, and P. Clifford, *Nucl. Instrum. Methods Phys. Res., Sect. A* **270**, 110 (1988); L. Lyons, A. J. Martin, and D. H. Saxon, *Phys. Rev. D* **41**, 982 (1990); A. Valassi, *Nucl. Instrum. Methods Phys. Res., Sect. A* **500**, 391 (2003).
- [29] R. Group, C. Ciobanu, K. Lannon, and C. Plager, in *Proceedings of the 34th International Conference in High Energy Physics (ICHEP08)*, Philadelphia, eConf C080730 (2008).